Case Studies in Construction Materials 17 (2022) e01495

Contents lists available at ScienceDirect

Case Studies in Construction Materials

journal homepage: www.elsevier.com/locate/cscm

Influence of sand grain size distribution and supplementary cementitious materials on the compressive strength of ultrahigh-performance concrete

Bassam A. Tayeh [a], Mahmoud H. Akeed [b], Shaker Qaidi [c,d], B.H. Abu Bakar [e,*]

[a] Civil Engineering Department, faculty of Engineering, Islamic University of Gaza, P.O. Box 108, Gaza Strip, Palestine
[b] School of Civil and Environmental Engineering, University of Technology Sydney (UTS), Sydney, Australia
[c] Department of Civil Engineering, College of Engineering, University of Duhok, Duhok, Kurdistan Region, Iraq
[d] Department of Civil Engineering, College of Engineering, Nawroz University, Duhok 42001, Iraq
[e] School of Civil Engineering, Engineering Campus, Universiti Sains Malaysia, Gelugor 11800, Penang, Malaysia

ARTICLE INFO

Keywords:
Ultrahigh-performance concrete
Compressive strength
Flowability
Fly ash
Microsilica

ABSTRACT

ultrahigh-performance concrete is a type of advanced concrete that can improve the resilience and durability of concrete structures. The utilization of available supplementary cementitious materials is a critical step in saving energy and materials, as well as lowering the cost of concrete. This research investigated the impact of sand grain size distribution, supplementary cementitious materials, and curing regimes (CRs) on the compressive strength of ultrahigh-performance concrete. The findings showed that a 90-d strength of 175 MPa could be obtained with a microsilica volume of 5 % and without heat-curing. The highest strength was obtained after curing for 48 h at 60 °C, followed by 72 h at 90 °C. Moreover, when compared to natural grain size distribution sand, the usage of finer sand enhances compressive strength. When microsilica is added, however, this impact is minimized.

1. Introduction

The advancement of supplementary cementitious materials, for instance, fly ash (FA) and microsilica, and chemical admixture, for instance, high-range water reducer, results in the creation of numerous varieties of high-quality concrete [1–8]. “High-strength concrete, high-performance concrete, and fiber-reinforced concrete are examples of these types of concrete. Further advancements in concrete technology have resulted in the creation of a new type of concrete known as ultrahigh-performance concrete. Ultrahigh-performance concrete is a cementitious composite having a tensile strength of 6 MPa and compressive strength of 150 MPa [9–13]. The age at which ultrahigh-performance concrete develops this strength is unknown. Several projects in Germany, the U.S, Canada, Australia, and France have proved the benefits of employing ultrahigh-performance concrete in the design of prestressed, precast concrete buildings [14–16]. Ultrahigh-performance concrete is primarily employed in bridge applications in the U.S, comprising prestressed, precast, precast waffle panels, bridge girders, and as a jointing material between precast concrete deck girders

Abbreviations: CR, Curing regimes; CS, Compressive strength; FA, Fly ash; GGBS, Ground Granulated Blast Furnace Slag; UHPFC, Ultra-high performance fiber concrete.

* Corresponding author.
E-mail address: cebad@usm.my (B.H.A. Bakar).

https://doi.org/10.1016/j.cscm.2022.e01495
Received 10 July 2022; Received in revised form 18 September 2022; Accepted 19 September 2022
Available online 20 September 2022
2214-5095/© 2022 The Author(s). Published by Elsevier Ltd. This is an open access article under the CC BY-NC-ND license (http://creativecommons.org/licenses/by-nc-nd/4.0/).

and panels" [17–19].

Because it comprised only exceptionally fine ingredients, ultrahigh-performance concrete was first known as reactive-powder concrete in the 1990s [20–23]. A typical ultrahigh-performance concrete mix contains cement, extra cementitious ingredients, fine sand, quartz, steel fiber, a high-range water reducer, and low water content [6,24–26]. Many ultrahigh-performance concrete mix proportions omit coarse aggregate. This exclusion lowers the number of microcracks in the coarse aggregate as well as in the ITZ between the coarse aggregate and paste matrix. These microcracks have the potential to improve the permeability of concrete. Furthermore, as the concrete resists external stresses, mechanical cracks form at the existing microcracks and spread through the coarse aggregate and paste matrix, potentially leading to concrete collapse. As a result, excluding coarse aggregate is required to increase the durability and strength of ultrahigh-performance concrete [27–29].

In terms of placement processes, "ultrahigh-performance concrete may decline the time and effort involved. Ultrahigh-performance concrete has rheological characteristics comparable to self-consolidating concrete. As a result, casting efforts are minimized, although more form preparation could be required [30–34]. The usage of a high-range water reducer is one of the primary variables leading to ultrahigh-performance concrete's great workability, whereas a low water content is required to obtain a high compressive strength. The water to binder ratio of ultrahigh-performance concrete could well be declined to 0.14" [20,35–42], where the binder is the entire content of cement and extra cementitious ingredients. Nevertheless, the needed w/c ratio for complete cement hydration is 0.33 [43,44]. The degree of hydration rises from 75 % to 95 % for standard concrete with a typical w/c ratio of 0.4. The water dosage of ultrahigh-performance concrete is so low that none of the cement particles are hydrated [45–47].

In several areas, ultrahigh-performance concrete is offered as a premix. "The premix needs specific care when blending, casting, curing, and testing. A high-shear mixer, for instance, is often required for blending ultrahigh-performance concrete, and a heat-curing process may be utilized to generate a high compressive strength. Ductal® is a commercialized type of ultrahigh-performance concrete created in collaboration with three companies: Rhodia, Lafarge, and Bouygues [48–52]. As a micro-filler ingredient, quartz powder with a Ø of 10 μm is utilized in the ultrahigh-performance concrete premix, which also comprises high tensile strength fibers" [23,52,53].

2. Research significance

Due to the advantages and challenges specific to the ultrahigh-performance concrete, additional studies are warranted. This paper aims to improve the understanding of ultrahigh-performance concrete by investigating the influences of sand grain size distribution, binder type and content, and CRs on concrete's compressive strength.

3. Experimental investigation

3.1. Materials

The binder for this investigation study is ordinary Portland cement Type I, densified microsilica, and Class C FA. Tables 1 and 2 lists the characteristics of cement-based materials. For the creation of ultrahigh-performance concrete, three grades of river sand were employed. Sand-A had a natural grain size distribution that ranged from the No. 4 sieve to the No. 200 sieve as shown in Fig. 1. Sand-B had lower particle sizes, passing the No. 30 filter but being held on the No. 50 screen as shown in Fig. 1. Another variety of sand (Sand-C) that passed sieve No. 200 was utilized to assess the impact of CRs on the compressive strength of concrete as shown in Fig. 1. Steel fiber made about 2.5 % of the total volume. The steel fibers were 13 mm in length and 0.25 mm in Ø, and the high-range water reducer admix was carboxylate-based. Moreover, the properties of the materials used in this investigation were within the scope of previous studies [54–57].

3.2. Testing procedure

Cube samples of 100 mm were cast to determine the compressive strength of concrete at 1, 7, 28, 56, and 90-d. The compression test was conducted in accordance with ASTM C 109 [58]. The load rate used was 1.3 MPa/s. After blending cement, sand, microsilica, and/or FA for 12 min, water and high-range water reducer additive were progressively added. Because of the high binder dosage and low water to binder ratio, all mixes required 12–25 min to mix. The concrete was then deposited without vibration in steel molds. After 1-d, the cubes were demolded and wet cured at 25 C till testing.

The flowability of fresh ultrahigh-performance concrete mixes was used to assess the rheology of the ultrahigh-performance concrete mixes. A flow table test was used to perform the flow test by ASTM C 1437 [59]. Flow tests were performed immediately

Table 1
Physical characteristics of cement-based materials.

Physical Characteristics	Specific area (cm^2/gm)	Mean grain size (μm)	Color	Initial setting (min)	Final setting (min)	Density (g/cm^3)	Specific gravity
Cement	3250	22.5	Dark Gray	45	360	3.15	2.2
Microsilica	150,000-300,000	0.15	Light to Dark Gray	–	–	2.21	3.1

Table 2
Chemical compositions of cement-based materials.

Compositions (%)	CaO	Al_2O_3	SiO_2	MgO	Fe_2O_3	Na_2O	K_2O	SO_3	LOI
Cement	63.61	5.04	20.25	4.56	3.16	0.08	0.51	2.1	3.13
Microsilica	0.7	1.12	85	0.8	1.46	0.8	1.056	–	< 6
FA	23.5	23.1	39.2	6.2	6.5	1.9	0.95	–	–

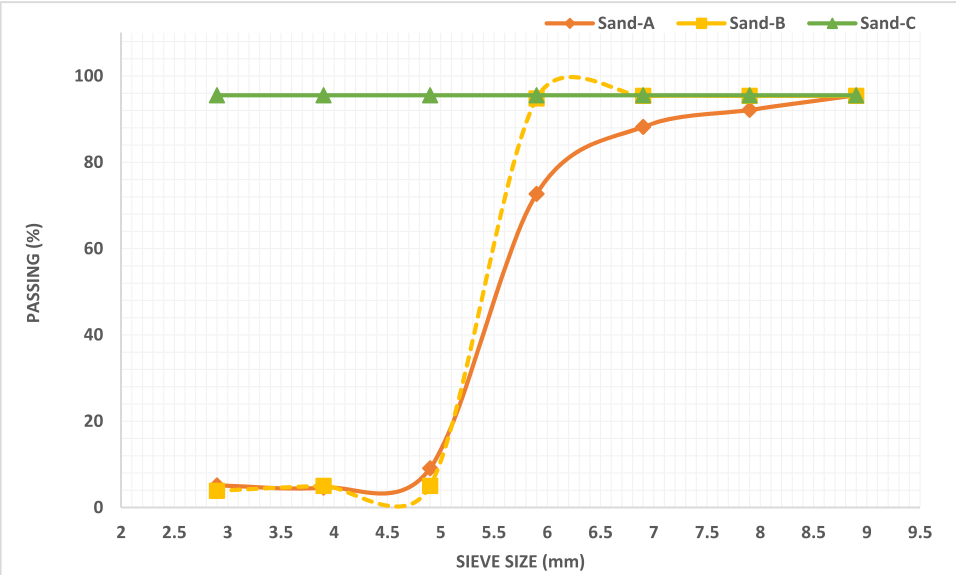

Fig. 1. Sand grain size distribution.

after the blending of each batch, and all mixes were evaluated twice.

Table 3 shows the proportions of the mix. To investigate the impact of microsilica on concrete compressive strength, microsilica was utilized at various percentages of 0, 7.5, 15, 20, and 25 % of the total binder content. The most effective microsilica content for ultrahigh-performance concrete would be determined by this broad range of microsilica substitutions. The FA content was 0, 30, 40, and 50 % by weight of the total binder content, respectively.

The CRs are also given in Table 3. For all ultrahigh-performance concrete mixes, CR I was utilized. Until the day of testing, this CR consisted of wet curing at 25 °C. M-16 I and II mixes were treated to three further CRs, II, III, and IV. For regimen II, the samples were cured for 5-d after casting at 75 °C and 95 % humidity before being examined. CR III included heat-curing at 100 % humidity for the first 5-d after curing. The temperature was 70 °C for the first 3-d and 100 °C for the final three. For the last CR, IV, the samples were

Table 3
Mixture proportions.

Mixture	Binder (kg/m^3)	water to binder ratio	Microsilica (%)	FA (%)	Steel fiber (%)	high-range water reducer kg/m^3	Sand	Curing regimes
M-1	920	0.23	–	–	–	34.6	Sand-A	I
M-2			–	–	–		Sand-B	I
M-3			7.5	–	–		Sand-A	I
M-4			15	–	–		Sand-A	I
M-5			20	–	–		Sand-A	I
M-6			25	–	–		Sand-A	I
M-7			7.5	–	–		Sand-B	I
M-8			–	30	–		Sand-A	I
M-9			–	40	–		Sand-A	I
M-10			–	50	–		Sand-A	I
M-11			5	30	–		Sand-A	I
M-12	1050		–	–	–	38.2	Sand-A	I
M-13			–	–	–		Sand-B	I
M-14			7.5	–	–		Sand-B	I
M-15			7.5	30	–		Sand-B	I
M-16-A	1410		25	–	–	51.3	Sand-C	I, II, III, and IV
M-16-B			25	–	2.5		Sand-C	I, II, III, and IV

cured at 25 °C and 90 % humidity for the first 7-d after casting, followed by 4-d at 100 °C and 100 % humidity.

4. Experimental findings and discussion

4.1. Flowability

Fig. 2 shows the findings of the measured flow of ultrahigh-performance concrete mixes. As can be observed, the fresh state characteristics alter dramatically with microsilica and sand grain size distribution addition. "Flow diameter variations were observed for composites formed from ternary blending of FA and microsilica. The declined workability of FA or microsilica-containing mixes can be attributed to an increase in calcium content and its rapid reactivity with the alkaline activator, where extra calcium served as nuclei for the precipitation of dissolved species from FA and impacted the coagulation rate"[31–33].

4.2. Compressive strength (CS)

Fig. 3 summarizes the CSs of mixes M-1 through M-15. Each CS value in the table is the average of three samples.

Fig. 4 depicts the impact of microsilica on the CSs of concrete. This graph shows the test findings for M-1, M-3, M-4, M-5, and M-6. Because all of these mixes included Sand-A, the comparison is valid. In general, regardless of the substitution rate, the usage of microsilica boosted strength at all ages. At 1, 28, 56, and 90-d, Mixture M-3 exhibited the highest CS. M-3 90-d CS was 10 % greater than the strengths of M-1, M-4, M-5, and M-6. At 1, 28, 56, and 90-d, the CS of M-3 was somewhat larger than that of M-4.

Fig. 4 further demonstrates the need of employing microsilica for ultrahigh-performance concrete mix percentage. At all ages, the CSs of M-1 are lower than those of M-3, M-4, and M-5. However, using too much microsilica had a detrimental impact on the CSs of the concrete. M-6 has higher CSs than M-1 but lower CSs than the other mixes. Several studies have demonstrated that when microsilica dosage rises, CS increases. "Curing circumstances may have contributed to this difference when compared to other investigations in the literature. The rate of pozzolanic reactions is slower in a wet curing state than in a heat-curing condition. Because all of the mixes in this series had low water to binder ratio and were cured at 25 °C and 100 % humidity until the day of testing when significant percentages of microsilica are utilized, a part of the microsilica stays unhydrated. When a high dosage of microsilica is employed, it cannot react with all of the available calcium hydroxides. As a result, the excess microsilica acts as a filler material without contributing to pozzolanic processes" [60,61].

Fig. 5 depicts the impact of various sand grain size distributions on the CSs of concrete. This graph covers the findings of M-1, M-2, M-3, and M-7. When comparing the findings of M-1 and M-2, using a finer Sand-B enhanced concrete CS, especially at later ages. "The maximum particle size in the paste matrix for M-2 is 650 μm, which is 10 times smaller than that of M-1. M-2 paste matrix is denser than the M-1 paste matrix, resulting in higher CSs. However, if the mixes included 5 % microsilica, the sand had no impact on the CSs. The impact is seen in the findings of M-3 and M-7 mixes". This discovery is due to microsilica potentially filling holes generated by the use of bigger sand particles and making the paste denser. The CSs of these two mixes were comparable after 90-d. The difference in maximum sand particle sizes between the four mixes is minor.

The compressive-strength values for mixes comprising Class C FA are shown in Fig. 6. The mixes shown in Fig. 6 are M-1 M-8, M-9,

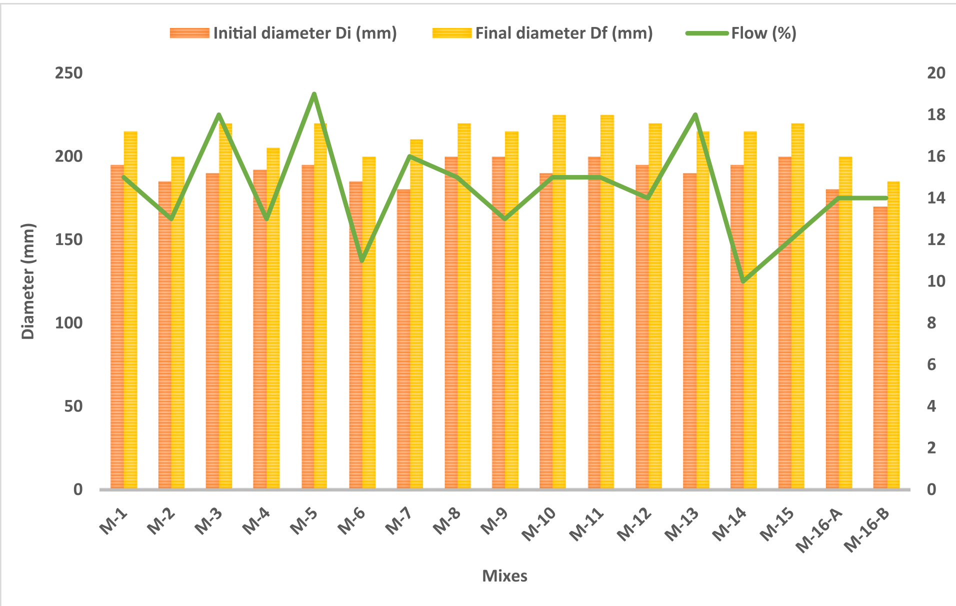

Fig. 2. Flow measurements of ultrahigh-performance concrete mixes.

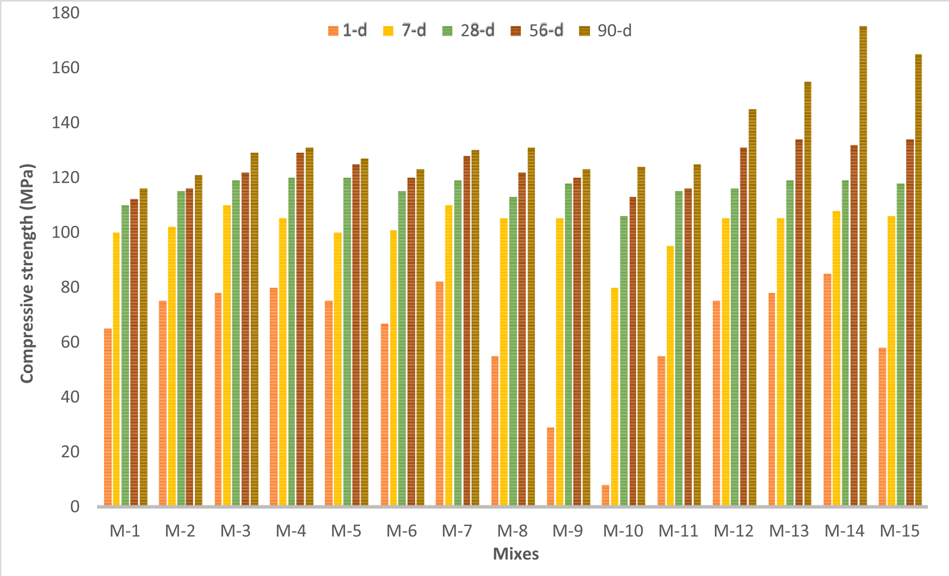

Fig. 3. CSs of the cube samples at different ages.

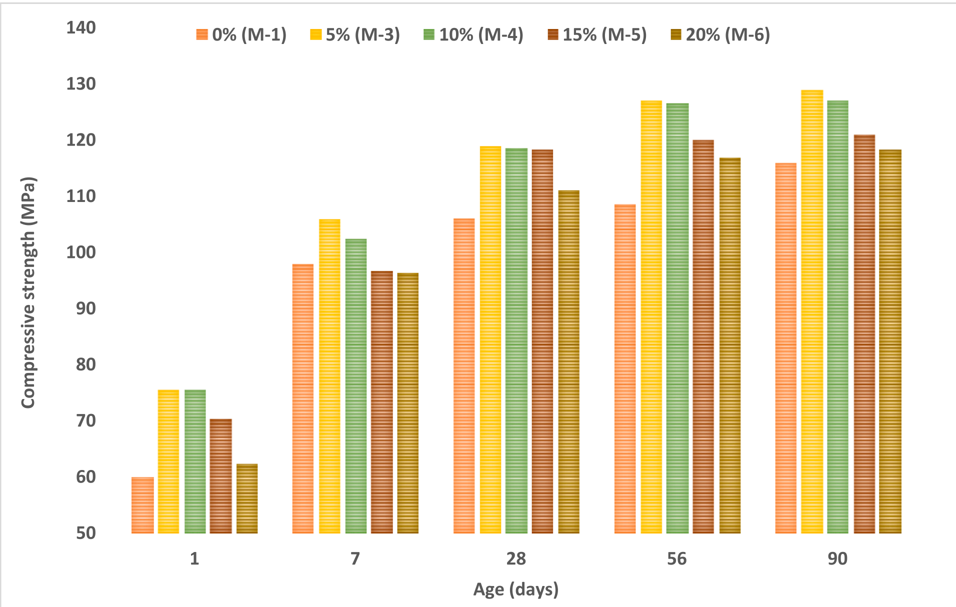

Fig. 4. The influence of microsilica on the CSs of concrete at various ages.

M-10, and M-11. "As seen in Fig. 6, when the FA percentage exceeds 30 %, the CS is lower than in mixes with a lower FA content. When compared to M-1, the 1-d strengths of M-8, M-9, M-10, and M-11 fell by 13 %, 65 %, 97 %, and 14%, respectively. The use of FA reduces the heat produced in the hydration process at early ages, and hence the strength. Concrete mixes containing FA develop substantial CS over time. The pozzolanic interactions of FA with calcium hydroxide produce C-S-H, which strengthens the paste matrix. At 28-d, the CSs of M-8 and M-9 are 5 % and 11 % higher, respectively, whereas M-10 is marginally weaker than M-1. M-8, M-9, and M-10 CSs were 5 %, 8 %, and 9 % stronger than M-1," respectively.

A FA percentage of 40 % generated the maximum CSs at 7, 28, 56, and 90-d of age, as illustrated in Fig. 5. M-9 mix percentage would be appropriate for concrete constructions where 1-d CS is not a concern or if heat-curing is a possibility. The 1-d CS of M-8 was 14 % lower than that of M-1, while the 90-d CS was 7 % higher. Furthermore, when comparing mixes of M-8 and M-11, the extra microsilica of 7.5 % in M-11 had no impact on the CS of the concrete, despite the fact that the findings of M-3 suggested a beneficial influence of microsilica. The pozzolanic reaction was achieved without the use of microsilica since the FA level was 30 %. The use of FA

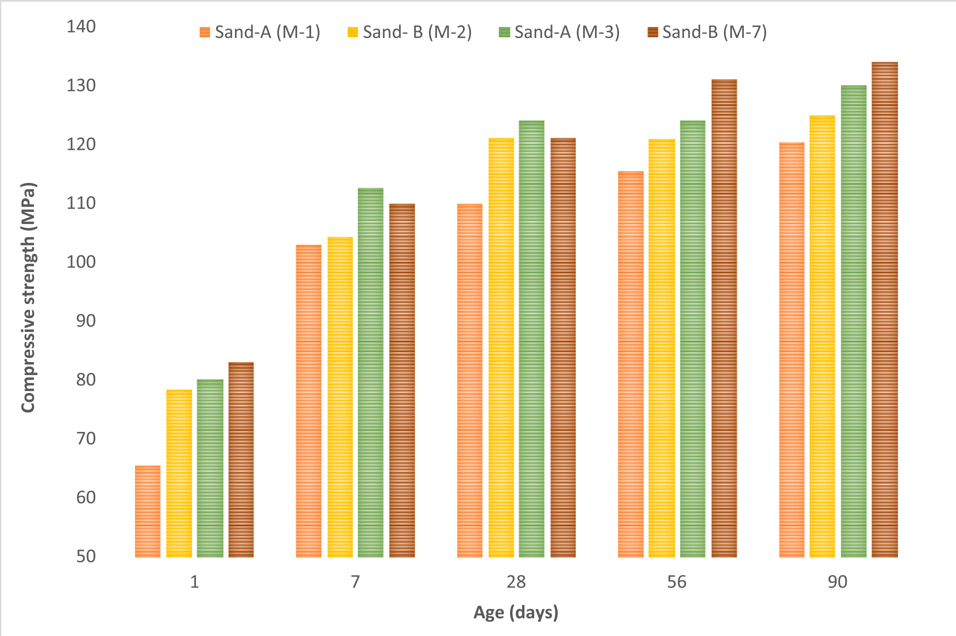

Fig. 5. The influence of Sand-A and Sand-B on the CSs of concrete.

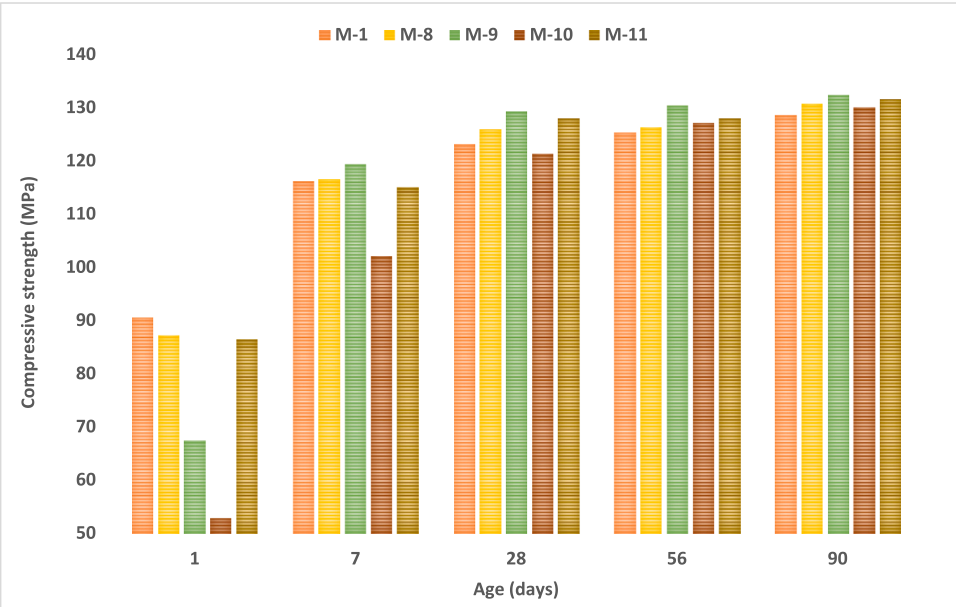

Fig. 6. The influence of FA on the CS of concrete.

and microsilica in the same ultrahigh-performance concrete mix percentage may reduce the influence of each component [9,37,44,62,63].

The link between the binder dosage and the CS of concrete is seen in Fig. 7. This figure comprises the findings of M-1, M-12, M-2, M-13, and M-7. As demonstrated in the figure, the CS of concrete improves as the total binder amount increases, independent of microsilica level or sand type. As the binder content increases, the paste matrix becomes stronger and can withstand larger compressive pressures. "Furthermore, with a water to binder ratio of 0.25, not all cement particles were hydrated, therefore the unhydrated cement particles enhanced the packing factor. The CSs of M-12 at 1, 7, 28, 56, and 90-d for concrete mixes comprising Sand-A were 27, 9, 11, 55, and 28 % larger than those of M-1, respectively. The sole difference between the two mixes was, once again, the binder content [10,20,35]. As the binder dosage of the concrete mixes comprising Sand-B, with or without microsilica, rose, so did the CS. M-14 has the

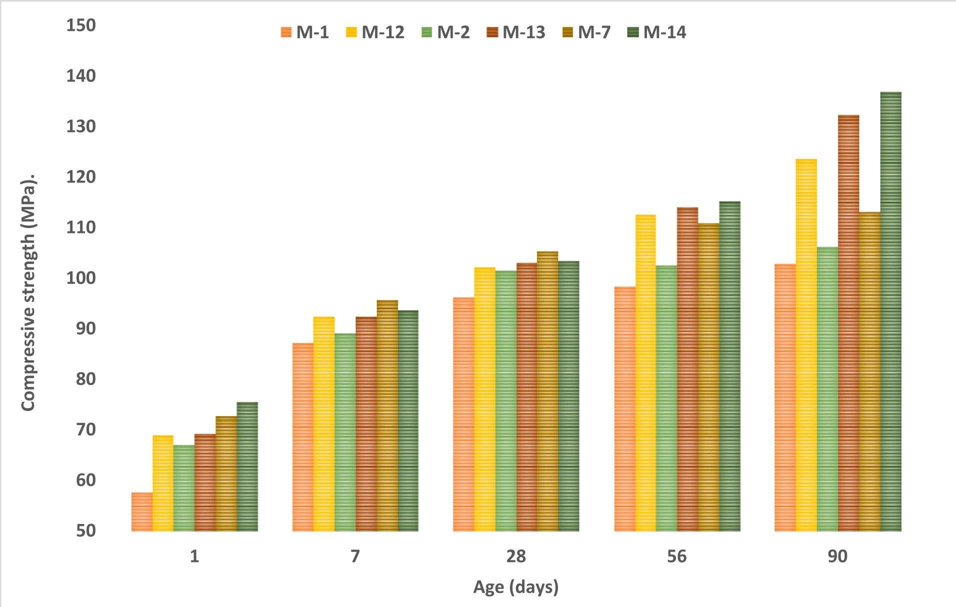

Fig. 7. The influence of binder content on the CSs of concrete at various ages.

greatest 90-d CS because of its high binder dosage, Sand-B, and 5% microsilica. M-15 carried an extra 30 % FA as compared to M-14. M-15's 1-d CS was 41 % lower than M-14's strength." This difference is attributable to the impact of FA on early strength development.

5. Conclusions

The following conclusions are drawn from the findings of this experimental investigation:

1. Ultrahigh-performance concrete mixes utilizing locally available ingredients can be created.
2. When compared to natural grain size distribution sand, the usage of finer sand enhances CS. When microsilica is added, however, this impact is minimized.
3. With a total binder of 1050 kg/m^3, 7.5 % microsilica, and Sand-A, a CS of 175 MPa was reached after 90-d.
4. The CS improves as the binder dosage increases, regardless of microsilica level or sand type.
5. A FA percentage of 40 % resulted in the maximum 90-d CS, whereas the content of 30 % had no impact on the strengths at any age.
6. A FA dosage of more than 40 % declined the CS of the concrete at early ages while increasing it at later ages.
7. The CRs impacted the CS of concrete. CR III produced the greatest CSs.

6. Future studies

In future research, it will be necessary to investigate the effects of other ratios different from those in this study, especially the size of sand grain size distribution, as well as other supplementary cementitious materials, on the performance of ultra-high performance mechanical concrete at full depth.

Declaration of Competing Interest

The authors declare that they have no known competing financial interests or personal relationships that could have appeared to influence the work reported in this paper.

Data availability

No data was used for the research described in the article.

Acknowledgment

The authors would like to acknowledge the school of civil engineering, Universiti Sains Malaysia, for funding the publication of this research paper. All authors have contributed equally to the conception and design of the study.

References

[1] M. Khan, M. Cao, A. Hussain, S.H. Chu, Effect of silica-fume content on performance of CaCO3 whisker and basalt fiber at matrix interface in cement-based composites, Constr. Build. Mater. 300 (2021), 124046.
[2] M. Cao, M. Khan, S. Ahmed, Effectiveness of calcium carbonate whisker in cementitious composites, periodica polytechnica, Civ. Eng. 64 (1) (2020) 265.
[3] M. Khan, M. Cao, C. Xie, M. Ali, Effectiveness of hybrid steel-basalt fiber reinforced concrete under compression, Case Stud. Constr. Mater. 16 (2022), e00941.
[4] M. Cao, M. Khan, Effectiveness of multiscale hybrid fiber reinforced cementitious composites under single degree of freedom hydraulic shaking table, Struct. Concr. 22 (1) (2021) 535–549.
[5] S. Arshad, M.B. Sharif, M. Irfan-ul-Hassan, M. Khan, J.-L. Zhang, Efficiency of supplementary cementitious materials and natural fiber on mechanical performance of concrete, Arab. J. Sci. Eng. 45 (10) (2020) 8577–8589.
[6] O. Smirnova, L. Kazanskaya, J. Koplík, H. Tan, X. Gu, Concrete based on clinker-free cement: Selecting the functional unit for environmental assessment, Sustainability 13 (1) (2020) 135.
[7] O. Smirnova, Low-clinker cements with low water demand, J. Mater. Civ. Eng. 32 (7) (2020), 06020008.
[8] O. Smirnova, D. Potyomkin, Influence of ground granulated blast furnace slag properties on the superplasticizers effect, Int. J. Civ. Eng. Technol. 9 (7) (2018) 874–880.
[9] S.M.A. Qaidi, D. Sulaiman Atrushi, A.S. Mohammed, H. Unis Ahmed, R.H. Faraj, W. Emad, B.A. Tayeh, H. Mohammed Najm, Ultra-high-performance geopolymer concrete: a review, Constr. Build. Mater. 346 (2022), 128495.
[10] M.H. Akeed, S. Qaidi, H.U. Ahmed, R.H. Faraj, S.S. Majeed, A.S. Mohammed, W. Emad, B.A. Tayeh, A.R.G. Azevedo, Ultra-high-performance fiber-reinforced concrete. Part V: mixture design, preparation, mixing, casting, and curing, Case Stud. Constr. Mater. 17 (2022), e01363.
[11] N. Zhang, C. Yan, L. Li, M. Khan, Assessment of fiber factor for the fracture toughness of polyethylene fiber reinforced geopolymer, Constr. Build. Mater. 319 (2022), 126130.
[12] M. Khan, M. Cao, H. Ai, A. Hussain, Basalt fibers in modified whisker reinforced cementitious composites, Periodica Polytech. Civ. Eng. 66 (2) (2022) 344–354.
[13] M. Khan, J. Lao, J.-G. Dai, Comparative study of advanced computational techniques for estimating the compressive strength of UHPC, J. Asian Concr. Fed. 8 (1) (2022) 51–68.
[14] S. Qaidi, Ultra-high-performance geopolymer concrete. Part 9: Strain hardening, University of Duhok, Duhok, 2022.
[15] S. Qaidi, Ultra-high-performance geopolymer concrete. Part 8: Dynamic behavior, University of Duhok, Duhok, 2022.
[16] S. Qaidi, Ultra-high-performance geopolymer concrete. Part 7: Mechanical performance correlation, University of Duhok, Duhok, 2022.
[17] B.A. Tayeh, B.A. Bakar, M.M. Johari, Y.L. Voo, Utilization of ultra-high performance fibre concrete (UHPFC) for rehabilitation – a review, Procedia Eng. 54 (2013) 525–538.
[18] A. Said, M. Elsayed, A. Abd El-Azim, F. Althoey, B.A. Tayeh, Using ultra-high performance fiber reinforced concrete in improvement shear strength of reinforced concrete beams, Case Stud. Constr. Mater. 16 (2022), e01009.
[19] W. Mansour, B.A. Tayeh, Shear behaviour of RC beams strengthened by various ultrahigh performance fibre-reinforced concrete systems, Advances in Civil Engineering 2020 (2020).
[20] M.H. Akeed, S. Qaidi, H.U. Ahmed, R.H. Faraj, A.S. Mohammed, W. Emad, B.A. Tayeh, A.R.G. Azevedo, Ultra-high-performance fiber-reinforced concrete. Part IV: –durability properties, cost assessment, applications, and challenges, Case Stud. Constr. Mater. 17 (2022), e01271.
[21] S.M.A. Qaidi, Ultra-high-performance fiber-reinforced concrete: Principles and raw materials, University of Duhok, Duhok, 2022.
[22] S.N. Ahmed, N.H. Sor, M.A. Ahmed, S.M.A. Qaidi, Thermal conductivity and hardened behavior of eco-friendly concrete incorporating waste polypropylene as fine aggregate, Materials Today: Proceedings (2022).
[23] S.M.A. Qaidi, B.A. Tayeh, H.F. Isleem, A.R.G. de Azevedo, H.U. Ahmed, W. Emad, Sustainable utilization of red mud waste (bauxite residue) and slag for the production of geopolymer composites: a review, Case Stud. Constr. Mater. 16 (2022), e00994.
[24] O. Smirnova, Development of classification of rheologically active microfillers for disperse systems with portland cement and super plasticizer, Int. J. Civ. Eng. Technol. 9 (10) (2018) 1966–1973.
[25] O.M. Smirnova, I. Menéndez Pidal de Navascués, V.R. Mikhailevskii, O.I. Kolosov, N.S. Skolota, Sound-absorbing composites with rubber crumb from used tires, Appl. Sci. 11 (16) (2021) 7347.
[26] Z. Saidova, G. Yakovlev, O. Smirnova, A. Gordina, N. Kuzmina, Modification of cement matrix with complex additive based on chrysotyl nanofibers and carbon black, Appl. Sci. 11 (15) (2021) 6943.
[27] S. Qaidi, Ultra-high-performance geopolymer concrete. Part 4: Mix design methods ‎, University of Duhok, Duhok, 2022.
[28] S. Qaidi, Ultra-high-performance geopolymer concrete. Part 3: Environmental parameters, University of Duhok, Duhok, 2022.
[29] M.T. Marvila, A.R.G. de Azevedo, P.R. de Matos, S.N. Monteiro, C.M.F. Vieira, Materials for production of high and ultra-high performance concrete: review and perspective of possible novel materials, Materials 14 (15) (2021) 4304.
[30] I. Almeshal, M.M. Al-Tayeb, S.M.A. Qaidi, B.H. Abu Bakar, B.A. Tayeh, Mechanical properties of eco-friendly cements-based glass powder in aggressive medium, Mater. Today.: Proc. 58 (2022) 1582–1587.
[31] Y.I.A. Aisheh, D.S. Atrushi, M.H. Akeed, S. Qaidi, B.A. Tayeh, Influence of steel fibers and microsilica on the mechanical properties of ultra-high-performance geopolymer concrete (UHP-GPC), Case Stud. Constr. Mater. 17 (2022), e01245.
[32] Y.I.A. Aisheh, D.S. Atrushi, M.H. Akeed, S. Qaidi, B.A. Tayeh, Influence of polypropylene and steel fibers on the mechanical properties of ultra-high-performance fiber-reinforced geopolymer concrete, Case Stud. Constr. Mater. 17 (2022), e01234.
[33] B.A. Tayeh, M.H. Akeed, S. Qaidi, B.H.A. Bakar, Influence of microsilica and polypropylene fibers on the fresh and mechanical properties of ultra-high performance geopolymer concrete (UHP-GPC), Case Stud. Constr. Mater. 17 (2022), e01367.
[34] A. Mansi, N.H. Sor, N. Hilal, S.M. Qaidi, The impact of nano clay on normal and high-performance concrete characteristics: a review, IOP Conference Series: Earth and Environmental Science, IOP Publishing, 2022, p. 012085.
[35] M.H. Akeed, S. Qaidi, H.U. Ahmed, W. Emad, R.H. Faraj, A.S. Mohammed, B.A. Tayeh, A.R.G. Azevedo, Ultra-high-performance fiber-reinforced concrete. Part III: fresh and hardened properties, Case Stud. Constr. Mater. 17 (2022), e01265.
[36] M.H. Akeed, S. Qaidi, H.U. Ahmed, R.H. Faraj, A.S. Mohammed, W. Emad, B.A. Tayeh, A.R.G. Azevedo, Ultra-high-performance fiber-reinforced concrete. Part II: hydration and microstructure, Case Stud. Constr. Mater. 17 (2022), e01289.
[37] M.H. Akeed, S. Qaidi, H.U. Ahmed, R.H. Faraj, A.S. Mohammed, W. Emad, B.A. Tayeh, A.R.G. Azevedo, Ultra-high-performance fiber-reinforced concrete. Part I: developments, principles, raw materials, Case Stud. Constr. Mater. 17 (2022), e01290.
[38] H. Unis Ahmed, L.J. Mahmood, M.A. Muhammad, R.H. Faraj, S.M.A. Qaidi, N. Hamah Sor, A.S. Mohammed, A.A. Mohammed, Geopolymer concrete as a cleaner construction material: An overview on materials and structural performances, Clean. Mater. 5 (2022), 100111.
[39] M.M. Al-Tayeb, Y.I.A. Aisheh, S.M.A. Qaidi, B.A. Tayeh, Experimental and simulation study on the impact resistance of concrete to replace high amounts of fine aggregate with plastic waste, Case Stud. Constr. Mater. (2022), e01324.
[40] F. Aslam, O. Zaid, F. Althoey, S.H. Alyami, S.M.A. Qaidi, J. de Prado Gil, R. Martínez-García, Evaluating the influence of fly ash and waste glass on the characteristics of coconut fibers reinforced concrete, Structural Concrete n/a(n/a).2022.
[41] F.A. Jawad Ahmad, Jesús de-Prado-Gil Rebeca Martinez-Garcia, M.A. Shaker, Ameni Brahmia Qaidi, Effects of waste glass and waste marble on mechanical and durability performance of concrete, Sci. Rep. 11 (1) (2021) 21525.
[42] H.U. Ahmed, A.A. Mohammed, S. Rafiq, A.S. Mohammed, A. Mosavi, N.H. Sor, S.M.A. Qaidi, Compressive strength of sustainable geopolymer concrete composites: a state-of-the-art review, Sustainability 13 (24) (2021) 13502.
[43] S.M.A. Qaidi, Ultra-high-performance fiber-reinforced concrete: Mixture design, University of Duhok, Duhok, 2022.
[44] S.M.A. Qaidi, Ultra-high-performance fiber-reinforced concrete: Hydration and microstructure, University of Duhok, Duhok, 2022.

[45] S. Qaidi, H.M. Najm, S.M. Abed, Y.O. Özkılıç, H. Al Dughaishi, M. Alosta, M.M.S. Sabri, F. Alkhatib, A. Milad, Concrete containing waste glass as an environmentally friendly aggregate: a review on fresh and mechanical characteristics, Materials 15 (18) (2022) 6222.

[46] B.A. Tayeh, M.H. Akeed, S. Qaidi, B.H.A. Bakar, Influence of the proportion of materials on the rheology and mechanical strength of ultrahigh-performance concrete, Case Stud. Constr. Mater. 17 (2022), e01433.

[47] A. Saeed, H.M. Najm, A. Hassan, S. Qaidi, M.M.S. Sabri, N.S. Mashaan, A. Comprehensive, Study on the effect of regular and staggered openings on the seismic performance of shear walls, Buildings 12 (9) (2022) 1293.

[48] S.M.A. Qaidi, Ultra-high-performance fiber-reinforced concrete: Durability properties, University of Duhok, Duhok, 2022.

[49] S.M.A. Qaidi, Ultra-high-performance fiber-reinforced concrete: Cost assessment, University of Duhok, Duhok, 2022.

[50] S.M.A. Qaidi, Ultra-high-performance fiber-reinforced concrete: Challenges, University of Duhok, Duhok, 2022.

[51] S. Qaidi, Ultra-High-Performance Fiber-Reinforced Concrete: Applications, Preprints (2022).

[52] S. Qaidi, Ultra-high-performance fiber-reinforced concrete (UHPFRC): A mini-review of the challenges, ScienceOpen Preprints.

[53] S.N. Ahmed, N. Hamah Sor, M.A. Ahmed, S.M.A. Qaidi, Thermal conductivity and hardened behavior of eco-friendly concrete incorporating waste polypropylene as fine aggregate, Mater. Today.: Proc. 57 (2022) 818–823.

[54] M.T. Marvila, A.R.Gd Azevedo, P.Rd Matos, S.N. Monteiro, C.M.F. Vieira, Rheological and the fresh state properties of alkali-activated mortars by blast furnace slag, Materials 14 (8) (2021) 2069.

[55] Y. Lv, L. Yang, J. Wang, B. Zhan, Z. Xi, Y. Qin, D. Liao, Performance of ultra-high-performance concrete incorporating municipal solid waste incineration fly ash, Case Stud. Constr. Mater. (2022), e01155.

[56] C.-q Wang, K. Liu, D.-m Huang, Q. Chen, M.-j Tu, K. Wu, Z.-h Shui, Utilization of fly ash as building material admixture: Basic properties and heavy metal leaching, Case Stud. Constr. Mater. 17 (2022), e01422.

[57] M.T. Marvila, A.R.G. de Azevedo, L.B. de Oliveira, G. de Castro Xavier, C.M.F. Vieira, Mechanical, physical and durability properties of activated alkali cement based on blast furnace slag as a function of% Na2O, Case Stud. Constr. Mater. 15 (2021), e00723.

[58] A.C. 109, Standard Test Method for Compressive Strength of Hydraulic Cement Mortar, ASTM International West Conshohocken, PA, USA.

[59] C. ASTM, Standard Test Method for Flow of Hydraulic Cement Mortar. C 1437, ASTM International West Conshohocken, 2007.

[60] S. Qaidi, Ultra-high-performance geopolymer concrete. Part 2: Applications, University of Duhok, Duhok, 2022.

[61] S. Qaidi, Ultra-high-performance geopolymer concrete. Part 1: Manufacture approaches, University of Duhok, Duhok, 2022.

[62] S.M.A. Qaidi, Ultra-high-performance fiber-reinforced concrete: Fresh properties, University of Duhok, Duhok, 2022.

[63] S.M.A. Qaidi, Ultra-high-performance fiber-reinforced concrete: Hardened properties, University of Duhok (UoD), 2022.